

Detection and Identification of Targets using Fusion of HSI and LiDAR Data

Deepti Yadav^a, M.K. Arora^a, K.C.Tiwari^b, J.K.Ghosh^a

^aIndian Institute of Technology, Roorkee, Uttarakhand 247667

Email:deepti.soni11@gmail.com, manoj.arora@gmail.com, gjkumfce@iitr,ernet.in

^bDelhi Technological University, Bawana Road, Delhi 110042

Email: kcchtpd@gmail.com

KEY WORDS: Target detection, target identification, hyperspectral, LiDAR, Fusion.

ABSTRACT:

A target in remote sensing may be defined as an object/activity of interest. Detection of targets is an essential requirement in numerous defence and civilian applications. Though primarily, the problem of target detection can be defined as a binary hypothesis testing problem which confirms the presence or absence of targets of interest, however, detection of a target itself may not be sufficient in decision making. Therefore, its classification and identification is also the key. Detection and identification of target using remote sensing data is a challenging task. Different remote sensing data such as hyperspectral (HSI), SAR, LiDAR data *etc.* have been used for detection of targets. Hyperspectral data, due to its high spectral information, has recently gained momentum in target detection but these may be limited to indicating presence of targets. Therefore, fusion of different datasets may be necessary. In this paper, an approach for detection and identification of two types of targets (vehicle and tree) using decision level fusion of HSI and LiDAR data has been proposed. Firstly, spectral detection using HSI data has been implemented. Next, LiDAR point cloud classification has been performed and used for computing morphological parameters for each target. Lastly the decisions obtained from HSI, LiDAR and morphological analysis have been fused to infer identity of desired targets. Results demonstrated that both types of targets have been successfully identified using the proposed approach.

1. INTRODUCTION

Resolving a target of interest using remote sensing data is one of the primary requirement in various applications/activities of military reconnaissance missions, intelligence, surveillance, traffic monitoring, disaster management and rescue operations *etc.* Such applications require information beyond mere detection of targets (Knox *et al.*, 2014; Puckrin *et al.*, 2012; Chang 2007). For example, for strategic planning in military combat intelligence applications, although it is important to confirm presence of the target but it is equally important to recognize the target, discriminate it from similar targets and also to know the count of the target. Such applications not only require to confirm presence of the target but also provide other details about the target and thus making target detection a more comprehensive process. The target detection process may also involve classification, discrimination, identification/recognition and quantification (Chang, 2007), as shown in Figure 1.

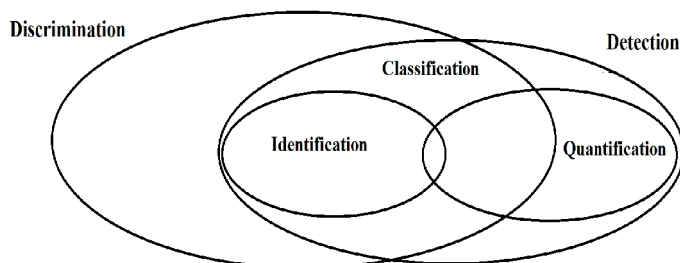


Figure 1: Target detection process

As seen from Figure 1, these processes are interrelated and thus can be used in conjunction with each other for more accurate target declaration. Target in remote sensing applications are often resolved on the basis of spectral and spatial characteristics of the target (Manolakis 2003), and contextual information is often used as supplementary information (Mahmoudi *et al.*, 2015; Guo *et al.*, 2013; Galleguillos *et al.*, 2010).

Over the years, detection and identification of targets based on the spectral or spatial properties has evolved significantly in terms of sensor technology and development of advanced algorithms. In the case of algorithms based on spectral properties, one of the major developments has been development of fine resolution hyper-spectral sensors capable of capturing data in several contiguous spectral bands thereby facilitating detection and identification of small targets. Detection using HSI however suffers from some issues such as dimensionality reduction, operational conditions existing in real time environment at the time of capture of data, such as variation in illumination, type of target, occlusion *etc.* (Dias *et al.*, 2013; Nasarbadi, 2014; Friman *et al.*, 2011; Manolakis 2003). Similarly in the case of analysis based on spatial properties, many algorithms based on spatial properties of target such as feature extraction, shape matching, object based recognition *etc.* have been reported in literature for target detection and identification (Borcs and Benedek, 2015; Varney and Asari, 2014; Sun *et al.*, 2013). These however are computationally intensive, require high resolution data, involve costly and target oriented data acquisition with small field of view. In addition, spatial properties are often dependent on target-sensor geometry. Therefore, uncertainties in real environment may induce variability in reflectance spectra or geometry of the target and thus may interfere with detection of targets. These may affect detection by either missing the target or by incorrectly detecting other objects as targets (false alarms). However, a target detection application often demands high accuracies. Literature suggests that accuracy of detection can be improved using fusion of data of different modalities. For instance, an algorithm based on spectral properties may declare a tree and shrub as same targets. However, spatial information in conjunction with spectral information can help to accurately distinguish such spectrally similar targets. Likewise, using only height may result in detecting some of the tree points into targets and may fail to distinguish targets with same height but of different materials. Therefore, fusion of supplementary/complementary data provided by multiple sources can produce better understanding of the area/target being investigated. Additionally, such detailed information enables detection as well identification of targets and thus improves the accuracy (Du *et al.*, 2013; Bigdeli *et al.*, 2013; Yun *et al.*, 2004).

Dalponte *et al.* (2012) performed fusion of HSI and LiDAR data for classification of tree species in Southern alps of Trento, Italy. They used hyperspectral data acquired using AISA Eagle sensor (having 126 band captured between 402.1 to 989.1 nm range and 1m spatial resolution), multispectral data obtained from GoeEye-1 satellite over area of interest (having four spectral band with 2 m spatial resolution and one panchromatic channel with 0.5 spatial resolution) and LiDAR data acquired using Optech ALTM3100EA (1m spatial resolution). Two combinations of datasets have been considered *i.e.* HSI with LiDAR and multispectral with LiDAR. Next, support vector machine and random forest classifier were used on both of the data combinations. Results demonstrated that higher accuracies were achieved using HSI-LiDAR datasets. Also, species of most of the trees could also be determined with this dataset. Thus, several studies have been reported for combined usage of HSI and LiDAR data for extraction of buildings, tree species identification, classification *etc.* (Tiede *et al.*, 2015; Park *et al.* 2013). These however have many limitations such as requirement of high point density LiDAR data, are computationally expensive and may not work for small targets *etc.*

In this paper, detection and identification of different types of targets have been performed using decision level fusion of hyperspectral data and LiDAR data. Detection has been performed using a popular detection algorithm namely Spectral Angle Mapper (SAM) for generating sufficiently accurate detection. Next for improving accuracy of detection, instead of exploring other suitable detection algorithms, an approach involving more thorough processing has been proposed. This approach includes a detection step and an identification step. The main idea is that any standard target detection algorithm will provide pixels belonging to target. These pixels however may also contain false alarms along with targets. Further an identification step has been applied. This involves extracting geometry of the target. The geometry has been compared with *a priori* available knowledge of the target. Lastly, a decision level fusion has been used for removing false alarms and confirming the identity of target with user visually examining all of the information obtained in comparison with *a priori* available knowledge of the target.

2. DATA

This study uses two different datasets *i.e.* co-registered hyperspectral (HSI) and LiDAR data, covering Rochester Institute of Technology (RIT) campus, New York. Both these datasets have been collected during a campaign (Herweg *et al.*, 2012) conducted by RIT in conjunction with SpecTIR, LLC during July 26 - 29, 2010. An orthorectified true color image of the area is shown in Figure 2(a). Two different types of targets, including natural and man-made targets *i.e.* tree and vehicle, have been considered.

2.1 Hyperspectral Data

Hyperspectral (HSI) data consisting of 360 bands ranging from 390 to 2450 nm with spectral resolution of 10 nm and spatial resolution of 1 m. It is captured using ProSpecTIR-VS2 sensor. From this data, a spatial subset of size 161 x 61 pixels covering region containing targets of interest has been generated. The targets considered include vehicle, tree, building and fabrics, as shown in Figure 2(b).

2.2 LiDAR Data

LiDAR point cloud captured using Leica ALS60 has also been used. It is co registered with HSI data. This data has spatial resolution of 1 m and average point density of 4 points per meter square. A subset of LiDAR point cloud covering the same area as that of hyperspectral subset has been used, as shown in Figure 2(c).

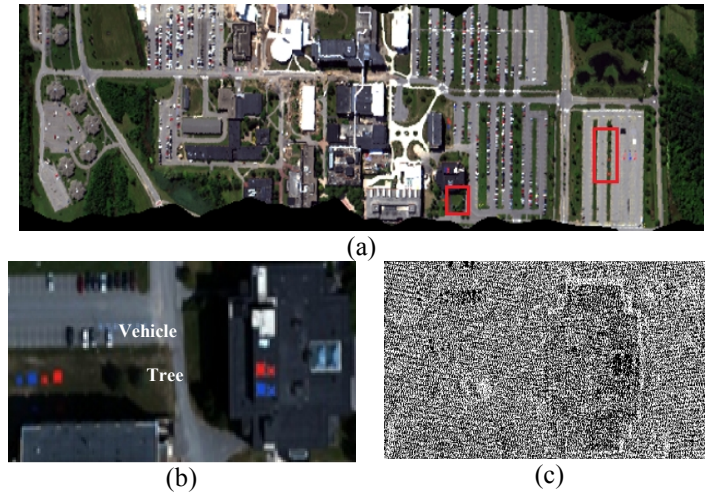


Figure 2: (a) Ortho-rectified true color image of RIT Campus (b) Hyperspectral image (c) LiDAR point cloud

2.3 Ground Truth Data

The ground truth database includes ground photos, positional measurement (latitude & longitude), 16 bit material reflectance spectrums (collected using ASD Field Spectro-radiometer) for each target. A high resolution RGB ortho-image of the study area has also been provided.

This study considers two different types of targets, as shown in Figure 3, *i.e.* a vehicle and a tree. Each target is different in terms of its shape and material composition etc. These diverse targets have been chosen for validating the effectiveness/generalization of proposed approach.



Figure 3: Ground photo of (a) Vehicle and (b) Tree

3. METHODOLOGY & IMPLEMENTATION

In remote sensing applications, targets can be differentiated by its material composition, placement, location and its shapes *etc.* These characteristics may help in detection and identification of the targets using different types of remote sensing data. In this paper, spectral as well as shape information about the target has been used for performing detection and identification of the target. The targets have been analyzed spectrally using hyperspectral data and geometrically (shape based) using LiDAR data. Lastly, detection and identification of different types of targets have been performed using decision level fusion of results obtained from hyperspectral and LiDAR data.

The approach developed involves a three step procedure. First, detection of target on hyperspectral data using Spectral Angle Mapper (SAM) has been performed. The detection of target pixels thus obtained has been referred to as potential target. The locations of these potential targets have been saved as seed locations for further processing. Second, LiDAR point cloud has been classified into five classes, namely, ground, building, vehicle, tree and fabric targets. These classes have been identified on the basis of *a priori* knowledge about the study area. Further, a class obtained from classification of LiDAR point cloud at seed locations of potential target is referred as potential target class. The LiDAR points, belonging to the potential target (as indicated from the detections in HSI), have been used to measure the morphological details of the target. The values obtained are then matched with morphological parameters of actual target. This has been done to retain only target points and discard false alarms.

Lastly, a decision level fusion, using results obtained from HSI processing and LiDAR processing, has been carried out for identification of each target. The work flow of methodology used for detection and identification of the desired targets is shown in Fig. 4.

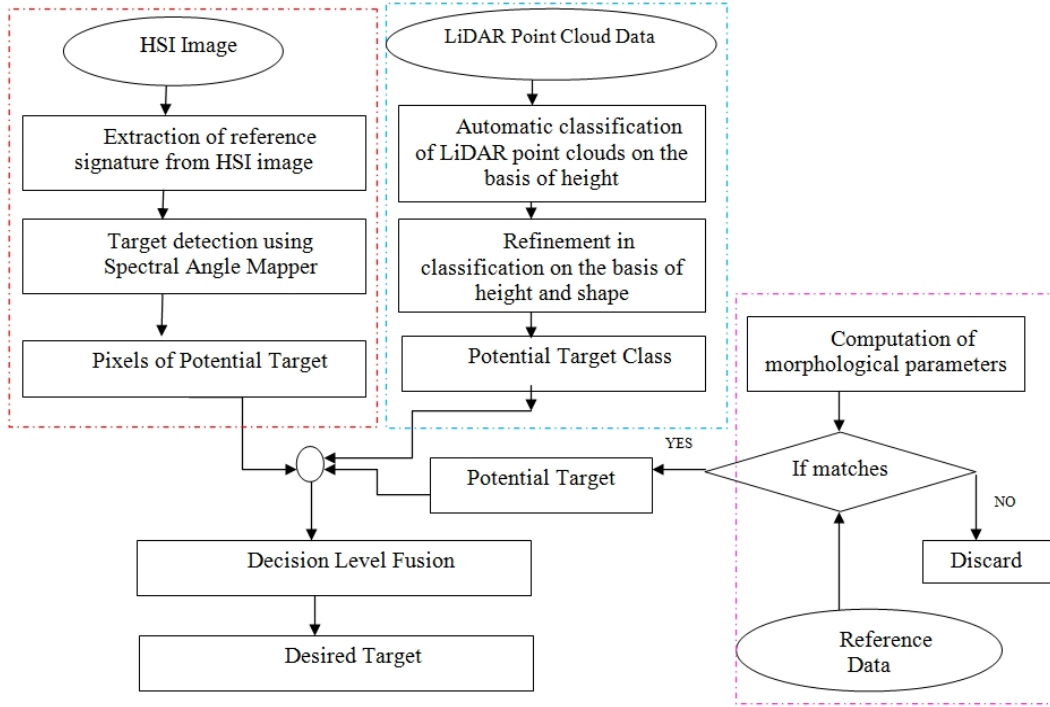


Figure 4: Flow chart of overall methodology

3.1 HSI Processing

In HSI, detection has been performed using Spectral Angle Mapper (SAM) algorithm. SAM has been chosen since it is invariant to illumination variations. SAM performs target detection by computing the cosine of angle between the spectrum of pixel under test and target reference spectrum. Value of the angle lies between zero and one (Kumar *et al.*, 2008; Chang *et al.*, 2001). Mathematically, it can be defined as,

$$T_{SAM} = \cos^{-1} \left[\frac{(\sum t_i r_i)}{(\sum t_i^2)^{1/2} (\sum r_i^2)^{1/2}} \right] \quad (1)$$

Where i is number of band, t_i = spectrum pixel under test and r_i = target reference spectrum. This is computed for each band. The algorithm compares each pixel spectrum with the reference spectrum. A smaller angle represents closer match to the reference spectrum. The computed angle is thresholded to generate a binary image indicating presence or absence of the target. The detections obtained using SAM provide pixels of desired targets. The locations of these potential targets have been considered during LiDAR processing.

3.2 LiDAR Data Processing

LiDAR point cloud has been processed in two steps. Step 1 involves classification of point cloud on the basis of height and shape of desired classes. Step 2 involves computation of morphological parameters of the target.

3.2.1 LiDAR point cloud Classification: In this step, LiDAR point cloud has been classified to locate and extract all 3D objects that exist in the entire area irrespective of the objects identity. It is done by processing range information of LiDAR data to delimit and isolate each of the individual 3D objects. LiDAR point cloud has been progressively classified into five user defined classes, namely, ground, building, vehicles, tree and fabric. These classes have been selected on the basis of *a priori* knowledge about features present in the study area. At each step, a set of LiDAR points are assigned to any one of these desired classes and classification of balance of the LiDAR

points is continued till all the points are assigned uniquely to one of the desired classes based on its height and 3-D shape.

Firstly, the points belonging to ground are separated from non ground points using progressive densification of triangulate irregular network (TIN) surfaces (Axelsson, 2000). In this method, lowest point in a grid of size 200 m has been chosen as initial ground points. Other ground points are then added to the initial set of points if their angle and distance to initial points is less than 6 degrees and 1.4 m respectively. These values have been fixed by trial and error. This is repeated till no other point meeting the criterion is left. Next, points belonging to building class have been classified from non ground points. For this, point which along with its neighbouring points forms a planar surface (representing roof) are considered for building class. The points belonging to surface with area greater than 40 m² are labelled as building points. This pre determined threshold is decided on the basis of knowledge about buildings in the study area. In addition, points considered for building class are checked for single echo return. Rest of the non ground points are classified into tree, vehicles and fabric class on the basis of height, intensity, contextual information and supervised visualization of its morphology/shape. Lastly, refinement in classification of each class is done by visually comparing the classified LiDAR cloud with a high resolution RGB orthoimage provided as reference data. This is done by overlapping the classified LiDAR cloud over a RGB orthoimage and manually correcting the misclassified points. LiDAR processing also helped on improving the accuracy of spectral detection obtained using HSI. This has been done by investigating each of the detection in classified LiDAR point cloud and removing false positives/detections. Before rejecting any potential target detected during spectral detection, its shape and height values were assessed with respect to that for each desired target. This helped in removing false alarms generated during spectral processing/detection.

At the end of this step, the presence and the location of the targets have been defined but a definite knowledge about their identity has not been investigated. In next step, the point cloud regions coincident with locations of potential targets detected in previous step are considered for further investigations.

3.2.2 Extraction of morphological parameters: This step is performed after LiDAR point cloud classification. Points belonging to previously selected regions are used to extract morphological information of the region. Several morphological parameters such as area, volume, rectangularity *etc.* have been used in several studies for detection and identification of targets (Aktaruzzaman *et al.*, 2010). In this paper, nine parameters have been used as descriptors of target structure/geometry and/or shape. These structural descriptors include length, width, height and contextual information, topological relation, structure, elevation profile. In addition, shape of the target is obtained using digital surface model and alpha shape. These have been used as for interpreting identity of the target. The parameters have been extracted by removing points of all other classes except the desired target and using the points of that class for measuring the parameters.

i. Dimensions (Length, width and height): The dimensions of the target class have been measured and compared with the dimensions of actual targets.

ii. Structure: It has been used to investigate whether the target is planar, linear or volumetric. For example, a road and a building, both made up of concrete but structurally a road is linear whereas a building has planar roof.

iii. Topological relation with ground has been measured to capture position of the target relative to the ground.

iv. Contextual information: It is defined as the information pertaining to target with respect to surrounding of the target (Mahmoudi *et al.*, 2015). Contextual information is not obtained directly by appearance of the target. It is obtained from surroundings of the target. Context may provide useful information for target recognition tasks (Guo *et al.*, 2013; Galleguillos *et al.*, 2010).

v. Elevation profile provides shape of the surface of the target and may aid in its identification.

vi. Digital surface model (DSM) is created using height of first return of LiDAR point cloud and therefore can be used to represent natural and built features. The DSM is generated by resampling the irregularly spaced LiDAR into regular spaced pixels. The size of pixel is an important factor which needs to be determined prior to resampling (Chang, 2008). Large pixel size may result in information loss and a very small value for pixel size may lead to redundancy. Literature suggests that optimum size of pixel can be approximated from mean point density of the LiDAR data.

In this study, a separate DSM has been generated for each target using points of the respective class and ground class only. This has been done to remove any distortion/confusion in shape with other classes. By comparing the DSM with *a priori* available/known shape of considered target, the identity of desired target has been established.

vii. Alpha shape can be used to represent shape of spatial point sets (Edelsbrunner *et al.*, 1983). Alpha shapes are generalizations of convex hull (Saeed *et al.*, 2013) and have been used in several researches for representing shapes of a desired object (Weygaert *et al.*, 2010). Here, alpha shapes have been used for representing shape of each of the target considered. For extracting alpha shape of target class, alpha radius has been set to 0.75 and 5 for vehicle and tree respectively.

3.3 Decision Level Fusion

In this experiment, hyperspectral and LiDAR data have been fused for detection and identification of different types of targets. A decision level fusion has been considered because it preserves the unique characteristics of both datasets and allows usage of appropriate algorithms for maximising the information obtained from each of the dataset (Shiomani, 2012; Kanaev, 2011). However, the ideal fusion method is highly application and data dependent (Pohl *et al.*, 1998). Mathematically, three sources of information *i.e.* S_1 , S_2 and S_3 has been used to obtain local decisions *i.e.* d_1 , d_2 and d_3 about identity of the target. The information obtained from local decisions d_1 , d_2 and d_3 have been fused to obtain overall decision D . The identity of target being investigated is obtained using D and *a priori* knowledge about target being investigated, as shown in Figure 5.

D -- Overall decision , S_i -- Source of information, d_i -- Local decisions

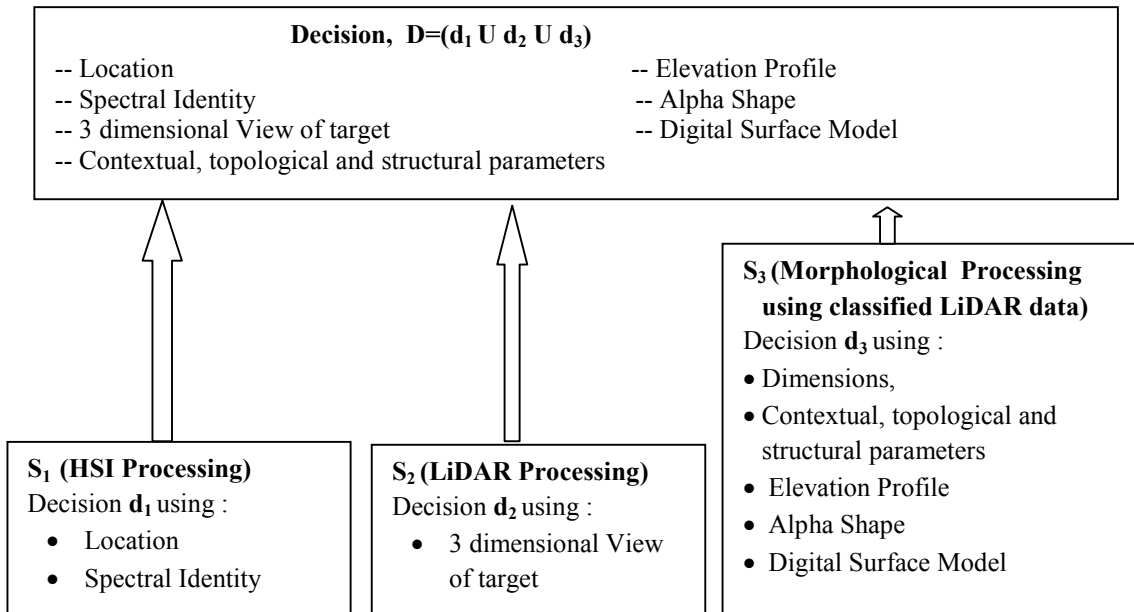


Figure 5: Decision Level Fusion

Therefore, the decision (D) about identity of potential target is taken on the basis of three sets of information such as spectral identity (obtained by spectral matching in HSI data) (d_1), visual analysis (obtained from three dimensional view generated in classified LiDAR point cloud) (d_2) and geometrical analysis (obtained by comparing computed morphological parameters with *a priori* knowledge) (d_3).

4. RESULTS & DISCUSSIONS

The detection and identification of targets have been implemented in three parts. The results of the implementations of each part have been discussed in following sections.

4.1 HSI Processing

Binary images obtained after implementing SAM for detection of vehicle, fabric targets, tree and building with their own reference spectra are shown in Figure 6(a), (b), (c) and (d) respectively.



(a) Vehicle target



(b) Tree target

Figure 6: Binary images depicting detection of vehicle and tree target using SAM

Following observations may be drawn from images in Figure 6,

1. Several pixels of the vehicle used for drawing the reference spectra have been detected. Besides, several other vehicles have also been detected (Figure 6 (a)). This may be due to the fact that *all* vehicles are quite similar in terms of material composition and thus reflectance properties.
2. Several pixels of the tree target have been detected (Figure 6(b)). In addition, pixels of other trees located in the scene have also been detected.

Therefore, HSI processing provides group of pixels for each target. Location of the most central pixel in each target has been extracted and used as seed location for further processing.

4.2 LiDAR Data Processing

Results obtained after LiDAR point cloud classification and morphological analysis have been discussed below,

4.2.1 LiDAR point cloud classification: The results of LiDAR point cloud classification is shown in Fig 7. All of the five pre defined classes namely ground, building, tree, vehicle and fabric were classified. Each of the class has been assigned a different color as shown in the legend in Fig. 7.

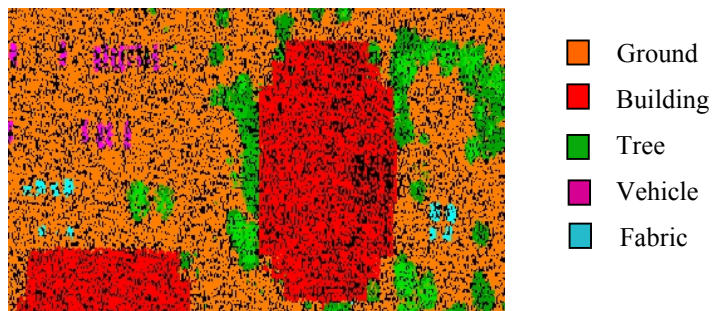


Figure 7: Classified LiDAR data

From visually inspecting the classification results, it may be observed that most of the points belonging to vehicle and tree class were delineated with the help of height difference of these points with respect to ground. Points of each target class have been considered for further processing.

4.2.2 Morphological analysis: In this step, LiDAR regions coincident with the locations of potential targets detected in HSI are considered for computation of nine morphological parameters. These parameters include length, width, height, context, topological relation, structure, elevation profile, digital surface model and alpha shape. The values obtained are summarized below:

i. Vehicle target: The values of the nine morphological parameters measured for vehicle target are summarized in Table 1.

Table 1: Morphological parameters of vehicle target class

<p>i) Length: 5.01 m ii) Width: 1.7 m iii) Height: 1.5 m iv) Context: placed on flat surface v) Topological relation: perpendicular to ground vi) Structure: Volumetric</p>	<p>vii) Elevation Profile</p>
<p>viii) Digital Surface Model</p>	<p>ix) Alpha shape</p>

The geometric properties have been used to support identification of the vehicles. In aerial imaging, vehicles forms rectangular shapes in different orientations and have a specific elevation profiles. Dimensions of few of the actual vehicles commonly used in the study *i.e.* New York, USA are summarized in Table 2.

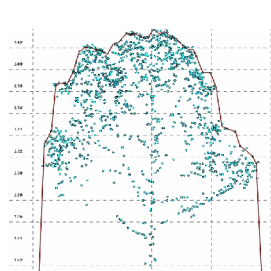
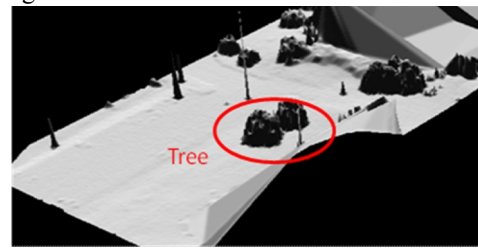
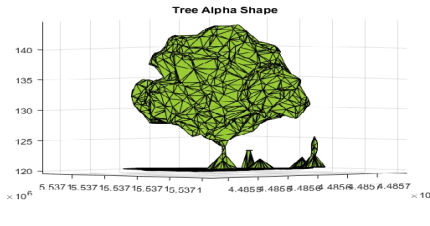
Table 2: Dimensions of actual vehicles

	Model	Length(m)	Width(m)	Height(m)
1	Potential Target (obtained from proposed method)	5.01	1.7	1.5
2	Kia Optima	4.85	1.855	1.47
3	Land Rover	4.59	1.91	1.72
4	Tesla	4.98	1.95	1.45
5	Toyota prius	4.45	1.75	1.47
6	Mercedes Benz	5.05	1.90	1.42
7	Cadiillac	4.72	1.85	1.42
8	BMW X5	4.87	1.94	1.76

The estimated dimensions (Table 1), have been compared with the actual dimensions of vehicles (Table 2). The dimensions of estimated vehicle have been found to be similar to actual vehicles like length of potential target is 5.01 m and average length of actual vehicles is 4.89 m . Visual analysis of elevation profile, DSM and alpha shape provided in Table 1 (vii, viii and ix) indicates identity of the target as a vehicle. Thus, on the basis of dimensional similarity and shape analysis, the potential target appears to be a car.

ii. Tree target: Table 3 summarizes the values of the parameters obtained for a tree target.

Table 3: Morphological parameters of tree target

<p>i) Length: 7.3 m ii) Width: 5.4 m iii) Height: 1.87 m iv) Context: placed on flat or elevated surface v) Topological relation: Perpendicular to ground vi) Structure: Volumetric</p>	<p>vii) Elevation Profile</p> 
<p>viii) Digital Surface Model</p> 	<p>ix) Alpha shape</p> 

The dimensions of a tree may vary. In fact, dimension of same tree may vary with each season. Therefore, dimensions cannot be used as reliable metric for comparison and identification of a tree. However, alpha shape, digital surface model have been used assessing the identity of potential target.

5.5.3 Decision Level Fusion: Identity of the targets have been established using decision level fusion of spectral and structural/morphological information obtained from HSI and LiDAR based analysis. For each of the targets considered, significant results/parameters contributing towards establishing identity of the target are summarized below,

i. Vehicle target: For inferring identity of potential vehicle target,

$\mathbf{d}_1 = \{\text{Location, Spectral Identity}\}$, $\mathbf{d}_2 = \{3 \text{ dimensional Shape}\}$ and $\mathbf{d}_3 = \{\text{Length, Width, Height, Alpha Shape, DSM, Elevation Profile, Topological Relation, Contextual, Structural parameter}\}$. Using $\mathbf{D}=(\mathbf{d}_1 \cup \mathbf{d}_2 \cup \mathbf{d}_3)$ along with *a priori* knowledge about target, the potential vehicle target has been identified as a car.

ii. **Tree:** The identity of potential tree target has been established using a computed decision $D=(d_1 \cup d_2 \cup d_3)$ where $d_1 = \{\text{Location, Spectral Identity}\}$, $d_2 = \{\text{3 dimensional Shape}\}$ and $d_3 = \{\text{Alpha Shape, DSM}\}$. Note that in case of tree and building targets, dimensions didn't contribute in decision making. This is because these targets may have varying dimensions and thus dimensions can't be used a reliable measure.

Therefore, the identity of each of the target have been detected and identified by performing decision level fusion using hyperspectral and LiDAR data. The benefit of shape information was shown to be a promising way to improve of spectral detection of targets in real operational environment. Further, the results obtained have been verified by comparing the locations of the detection with a priori known location of the targets. Location of centre most pixel of the target have been extracted for the purpose of comparison as summarized in Table 6.

Table 6: A comparison of locations of targets obtained and that available from reference data

Name of Target	Location of Target(from Results) (latitude/longitude)	Location of Target(from Reference data) (latitude/longitude)
Vehicle (centre most pixel)	281981.43 N, 4773838.08 W	281985.48 N, 4773839.85 W
Tree (centre most pixel)	281985.47 N, 4773825.58 W	281986.83 N, 4773828.67 W

5. CONCLUSIONS

The efficacy proposed approach for detection and identification of different types of targets using decision level fusion of hyperspectral and LiDAR data was demonstrated in this paper. The method implemented for detection and identification of targets performs spectral analysis using HSI data followed by structural analysis using LiDAR data. Results obtained demonstrated the potential of the approach for detection and identification of both of the target of different shapes and composition. It has been found that *a priori* known volumetric target such as vehicle, trees can be accurately identified using this approach. However, identification of targets with very low height with respect to ground can be challenging.

Therefore combined usage of HSI and LiDAR data provide additional information about targets and future work will focus on investigating potential of the proposed technique for identification of targets with very low height with respect to ground and also to perform identification in presence of clutter, illumination variance, and occlusion.

REFERENCES

- Aktaruzzaman, M. D. and Schmitt, T. G. 2010. Detailed digital surface model DSM generation and automatic object detection to facilitate modelling of urban flooding. ISPRS Archives, High-Resolution Earth Imaging for Geospatial Information, , Hannover, Germany, Volume XXXVIII-1-4-7/W5, June 2-5, 2009.
- Axelsson, P. 2000 . DEM generation from laser scanner data using adaptive tin models. Int. Arch. Photogramm. Remote Sens., Vol. 33, pp.111–118, 2000.
- Bigdeli, B., Samadzadegan, F. and Reinartz, P. 2013. Classifier fusion of hyperspectral and LIDAR remote sensing data for improvement of land cover classification. International Archives of the Photogrammetry, Remote Sensing and Spatial Information Sciences, Vol. 40, pp. 97-102. Iran. Oct.13
- Bores A. and Benedek C. 2015. Extraction of vehicle groups in airborne LiDAR point clouds with two-level point processes. IEEE Trans. Geosci. Remote Sens., vol. 53, no. 3, pp. 1475–1489, Mar. 2015.
- Chang Y. C., Habib A.Y., Lee D.C. and Yom J.H. 2008. Automatic Classification of LiDAR Data Into Ground and NonGround Points. International Archives of the Photogrammetry, Remote Sensing and Spatial Information Sciences, Beijing, China, Vol. XXXVII, Part B4, 2008
- Chang, C.I. 2007. Hyperspectral Data Exploitation. Hoboken, New Jersey: John Wiley& Sons.
- Chang, C.I., Ren, H. and Chiang, S. S. 2001. Real-time processing algorithms for target detection and classification in hyperspectral imagery. Geoscience and Remote Sensing, IEEE Transactions, Vol. 39, pp. 760-768.
- Dalponete M., Bruzzone L., Gianelle D. 2012. Tree species classification in the Southern Alps based on the fusion of very high geometrical resolution multispectral/hyperspectral images and LiDAR data. Remote Sensing of Environment, 123: 258-270.
- Dias J. M B., Plaza A. and Valls G. C. 2013. Hyperspectral Remote Sensing Data Analysis and Future Challenges. IEEE Geoscience and remote sensing magazine, pp.6-36, 2013.
- Du, P., Liu, S., Xia, J., Zhao, Y. 2013. Information fusion techniques for change detection from multi-temporal remote sensing images. Information Fusion, 14, pp. 19-27.
- Edelsbrunner, H., Kirckpatrick D. G., and Seidel R. 1983. On the shape of a set of points in the plane. IEEE Transaction on Information Theory, IT-29, pp. 551-559.

- Friman, O., Tolt, G. and Ahlberg, J. 2011. Illumination and shadow compensation of hyperspectral images using a digital surface model and non-linear least squares estimation. *Image and Signal Processing for Remote Sensing. Proc. of SPIE*, 2011. 81800Q-1: 8.
- Galleguillos C., McFee B., Belongie S., and Lanckriet G. R. G. 2010. Multi-class object localization by combining local contextual interactions. *Computer Vision and Pattern Recognition CVPR*, 2010
- Guo, J., Zhou, H. and Zhu, Ch. 2013. Cascaded classification of high resolution remote sensing images using multiple contexts. *Inf. Sci.*, Vol. 221, no. 2013, pp. 84–97.
- Herweg, J.A., Kerekes, J.P., Weatherbee, O., Messinger, D., Aardt, J.V., Ientilucci, E.J., Ninkov, Z., Faulring, J., Raqueño, N. and Meola, J. 2012. SpecTIR Hyperspectral Airborne Rochester Experiment Data Collection Campaign. *Proc. of Algorithms and Technologies for Multispectral, Hyperspectral, and Ultraspectral Imagery XVIII, SPIE, USA*, Vol. 8390.
- Kanaev A. V., Daniel B. D., Neumann J.G., Kim, A. M. and Lee K. R. 2011. Object level HSI-LIDAR data fusion for automated detection of difficult targets. *Optics Express*, Vol. 19, No. 21.
- Knox, M., Tatum, S. and Collins, L. 2014. Target detection and identification using synthetic aperture acoustics. *Proc. SPIE 9072, Detection and Sensing of Mines, Explosive Objects, and Obscured Targets XIX*, 907206 May 29, doi:10.1117/12.2050390.
- Kumar, U. and Ramachandra, T.V. 2008. End members discriminations in MODIS using spectral angle mapper and maximum likelihood algorithms. *International Journal of Applied Remote Sensing*, Vol. 2, no. 1, pp. 1-14.
- Mahmoodi A., Bang D., Olsen K., Zhao Y. A., Shi Z., Broberg K., Safavi S., Han S., Ahmadabadi M. N., Frith C. D., Roepstorff D., Rees G. and Bahrami D. 2015. Equality bias impairs collective decision-making across cultures. *PNAS* 2015 112 12 3835-3840; published ahead of print March 9, 2015, doi:10.1073/pnas.1421692112.
- Manolakis, D., Marden, D. and Shaw, G.A. 2003. Hyperspectral image processing for automatic target detection applications. *Lincoln Laboratory Journal*, vol.14 1, pp.79–115.
- Nasrabadi N.M. 2014, Hyperspectral Target Detection: An Overview of Current and Future Challenges. *Signal Processing Magazine, IEEE*, Vol. 311, pp. 34-44, Jan 2014.
- Park, S.E., Yamaguchi, Y. and Kim, D.J. 2013. Polarimetric SAR remote sensing of the 2011 Tohoku earthquake using ALOS/PALSAR. *Remote. Sens. Environ.* May, Vol. 132, pp. 212-220.
- Pohl, C. and Van Genderen, J. L. 1998. Multisensor image fusion in remote sensing: concepts, methods and applications. *International Journal of Remote Sensing*, Vol.19, pp. 823-854.
- Puckrin, E., Turcotte, C. S., Gagnon, M., Bastedo, J., Farley, V. and Chamberland, M. 2012. Airborne infrared hyperspectral imager for intelligence, surveillance and reconnaissance applications. *Proc. of SPIE*, doi:10.1117/12.918251.
- Saeed A., Farzad D. Ali M. 2013. Alpha-Concave Hull, a Generalization of Convex Hull. eprint arXiv:1309.7829, September 2013.
- Shimoni, M., Tolt, G., Perneel, C. and Ahlberg J. 2011. Detection of Vehicles in Shadow Areas using Combined Hyperspectral and LIDAR Data. *IEEE Transactions on Geoscience and Remote Sensing*, Vol. 6, No. 11.
- Sun, S. and Salvaggio, C. 2013. Aerial 3D Building Detection and Modeling from Airborne LiDAR Point Clouds. *IEEE Journal of Selected Topics in Applied Earth Observations and Remote Sensing*, Vol.6, 3 June, pp 1440-1449.
- Tiede D., Oltmanns S. O., Baraldi A. 2015. Geospatial 2D and 3D object-based classification and 3D reconstruction of ISO-containers depicted in a LiDAR data set and aerial imagery of a harbor. *IEEE International Geoscience & Remote Sensing Symposium*. pp. 4181-4184.
- Varney, N.M. and Asari, V.K. 2014. Volumetric features for object region classification in 3D LiDAR point clouds. *IEEE Applied Imagery Pattern Recognition Workshop AIPR*, Washington DC, 14- 16 Oct, pp.1 – 6.
- Weygaert, R., Platen, E., Vegter, G., Eldering, B. and Kruithof, N. 2010. Alpha shape topology of the cosmic web. In *Voronoi Diagrams in Science and Engineering ISVD*, 2010 IEEE International Symposium, pp. 224–234.
- Yun Zhang. 2004. Understanding Image Fusion. *Photogramm. Eng. Remote Sens.* 657-661.